

Terahertz-Emitting Silicon-Germanium Devices

Ralph T. Troeger, Thomas N. Adam, Samit K. Ray, Pengcheng Lv, Ulrike Lehmann, and James Kolodzey

Department of Electrical and Computer Engineering, University of Delaware,
Newark, DE 19716, U.S.A.

ABSTRACT

In this paper we report on far-infrared emission in the 1-12 THz frequency range from strained SiGe structures. Pseudomorphic superlattices were grown by Molecular Beam Epitaxy (MBE) at the relatively low substrate temperature of 400°C to prevent germanium segregation. Layer thicknesses, composition, and crystallinity were confirmed by high-resolution X-ray diffraction. Devices were designed to produce confined hole states with various energy separations. Mesa devices were etched in a reactive-ion etching system and tested for edge emission over a wide range of drive currents using an FTIR spectrometer in step-scan mode. THz emission was observed in pulsed mode at current densities as low as 50 A/cm² and at temperatures as high as 50 K, using a liquid-helium-cooled silicon bolometer detector with a lock-in amplifier. Emission spectral peaks occurred at 7.9 and 9.36 THz for two different samples, in good agreement with k-p calculations.

INTRODUCTION

Recently, emitters and detectors operating in the terahertz gap of the electromagnetic spectrum (0.3-30 THz, 1000-10 μm wavelength) have garnered much interest for possible application in such fields as ranging [1], imaging [2, 3], gas and environmental sensing [4, 5], wireless communications [6], and spectroscopy [7]. Quantum cascade lasers (QCL) fabricated from III-V materials have demonstrated light emission at wavelengths typically below 10 μm [8] over a relatively large temperature range [9]. However, these devices are thought to be severely limited within the THz range due to strong reststrahlen absorption in III-V compound semiconductors [10]. Fabricating THz light emitters based on the SiGe material system would not only circumvent this problem due to the absence of such absorption bands in SiGe, but also enable production of opto-electronic devices compatible with Si CMOS technology. A number of such structures have recently been reported.

Stimulated THz emission was demonstrated from boron delta-doped sheets located within strained SiGe quantum wells at a wavelength of approximately 100 μm [11]. The optical transition in these structures is between acceptor states in the band gap, which are split by the built-in strain. Electroluminescence has also been reported from structures based on intersubband transitions between confined states in SiGe quantum wells. The observed emission was typically at the upper limit of the THz range, with emission reported at for instance 30 THz [12] and 34-37 THz [13]. A few reports on longer-wavelength emission at 2.9 and 6 THz have been published [14, 15].

In this paper we report on measurements of THz electroluminescence from strained SiGe quantum well structures and its dependence on the pumping conditions.

THEORY

In the SiGe material system, band gap difference manifests itself mainly as offset in the valence band. Quantum well devices fabricated from SiGe alloys do therefore most frequently employ the confinement of holes in the valence band.

A number of factors complicate theoretical calculations for such structures. Quantum wells in the valence band may confine heavy holes, light holes, and spin-orbit split-off holes. The spin-orbit interaction splits the valence bands into a four-fold and a two-fold degenerate band. SiGe alloys on Si substrates are typically strained, resulting in additional splittings of the band edges and coupling between different valence bands. For calculations to be accurate, all these effects have to be taken into account.

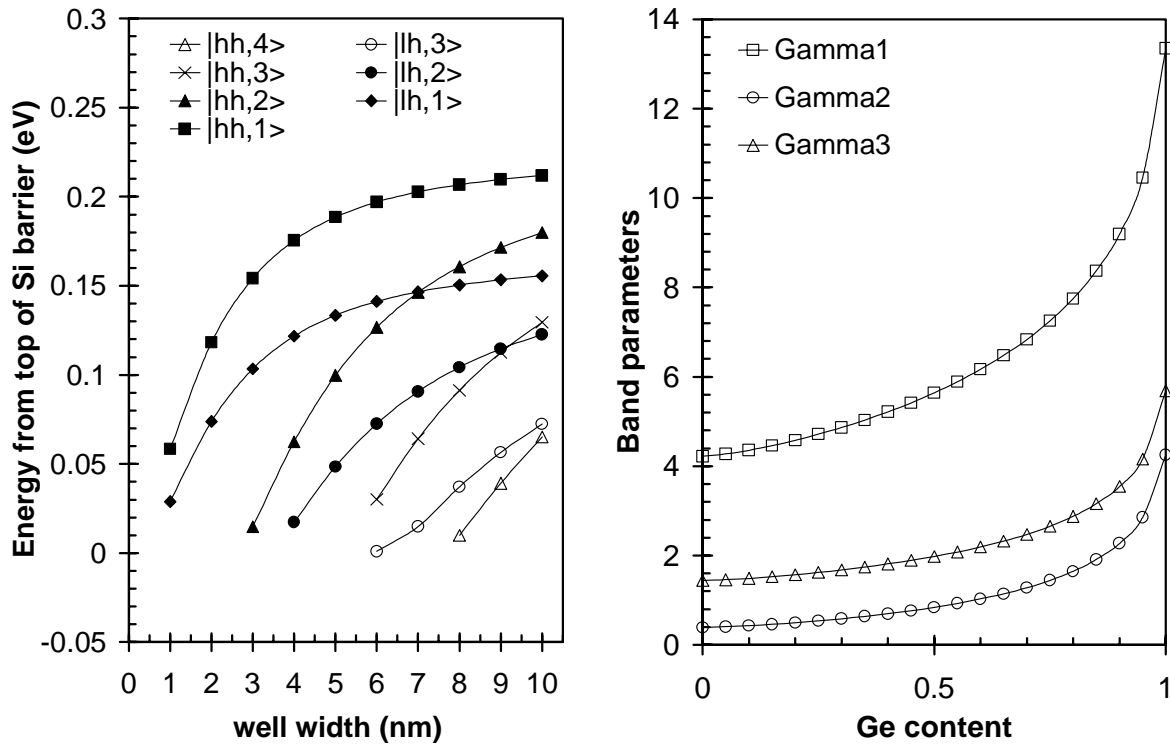


Figure 1: Left: Calculated eigenenergies of confined states in a Si/Si_{0.7}Ge_{0.3}/Si quantum well vs. well width for zero applied electric field. Energy is taken with respect to the heavy hole/light hole band edge in the Si barrier. The bottoms of the heavy hole and light hole quantum wells occur at 223 meV and 167 meV, respectively. **Right:** Luttinger hole mass parameters used for calculations.

We have calculated the confined state energies for quantum wells with varying well widths and germanium contents using a commercially available k-p software package [16]. Applied static electric fields can be taken into account in the calculations. Elastic constants, valence band deformation potentials, spin-orbit splittings, and lattice constants for SiGe layers have been calculated by linearly interpolating between the values for Si and Ge. To determine the valence band parameters, non-linear interpolation according to Rieger and Vogl [17] has been carried out. We have corrected the adjustable parameters in the interpolation expression for better fit of

experimental values for pure Si and Ge. The Luttinger parameters for a SiGe alloy as a function of Ge content are given in Figure 1.

Confined state energies for zero external electric field for a $\text{Si}_{0.70}\text{Ge}_{0.30}$ quantum well as function of the quantum well width are also summarized in Figure 1. For small quantum well widths, the wells will only have two confined states; one heavy-hole state; and one state that has both spin-orbit and light-hole character. We have selected well widths for this Ge content that have different separations in energy corresponding to transitions slightly below 10 THz.

EXPERIMENT

Two different 16-period SiGe/Si superlattice samples were grown by solid source Molecular Beam Epitaxy (MBE) at a substrate temperature of 400°C to minimize the effects of Ge segregation [18]. The substrate preparation and growth process are described elsewhere in detail [19]. Si was evaporated using an e-beam evaporation source, while Ge was evaporated from a standard effusion cell. The growth rate was on the order of 2 Å per minute. In-situ Reflection-High Energy Electron Diffraction (RHEED) observations and high-resolution X-ray diffraction confirmed crystallinity, strain, layer thicknesses, and compositions. Sample SGC396 had 16 Å thick wells, whereas sample SGC420 had quantum wells approximately 13.5 Å thick. The germanium concentration in the wells of both samples was 30%. With the exception of a Si cap which in SGC420 was doped with boron to a concentration of $5 \times 10^{18} \text{ cm}^{-3}$, the structures were not intentionally doped.

For SGC420, mesas 100 μm by 1850 μm in area and approximately 17 μm deep were fabricated using a multi-step reactive ion etching (MSRIE) process [20]. Metal contacts consisting of 200 Å Ti, 200 Å Pt, and 5000 Å Au were deposited using e-beam evaporation and standard lift-off technique. For sample SGC396, a metal finger pattern 50-150 μm wide consisting of 200 Å Ti/2500 Å Au was deposited directly on the sample surface using a lift-off technique without etching. The fingers were spaced 70-350 μm and connected to a large common bond pad. The device area for this sample was approximately 1 cm². For both samples, a large-area backside contact was achieved by evaporating Ti/Pt/Au or Ti/Au for SGC420 and SGC396, respectively.

Both samples were mounted onto copper sample holders using thin indium sheets or conductive epoxy. The sample holders were then attached to the cold finger of an open-loop liquid helium cryostat. The metal pads were contacted by wedge bonding Au wires to them.

Electroluminescence spectra were measured in edge-emission geometry by Fourier Transform Infrared Spectroscopy (FTIR) using a Nicolet Nexus860 spectrometer or a Nexus870 spectrometer for SGC396 and SGC420, respectively. The measurements were performed in amplitude modulation step-scan mode with a liquid-helium cooled Si bolometer as detector used in combination with a lock-in amplifier. During the measurement of SGC396, bursts of 800 ns pulses of 54 V were applied to the sample at a repetition rate of 413 Hz. For SGC420, bursts of 500 ns pulses were applied with a similar repetition rate, and spectra were taken at different sample voltages. Duty cycles were chosen to prevent sample heating during the measurement, which would produce broadband black body radiation. The lock-in amplifier was tuned to the pulse train repetition frequency.

RESULTS AND DISCUSSION

Electroluminescent spectra from SGC396 and SGC 420 taken at a sample temperature of 5K are depicted in Figure 2. We observed peaks in the spectra which center at 9.36 and 7.9 THz for SGC396 and SGC420 respectively. For SGC420, the intensity of the electroluminescence increases linearly with applied pumping current density.

The observed electroluminescence is centered on frequencies that agree well with the results of k-p calculations as depicted in Figure 3, suggesting emission from confined states in the quantum wells. The observed emission frequency, however, also corresponds to dopand emission bands, which may play a role in the observed emission.

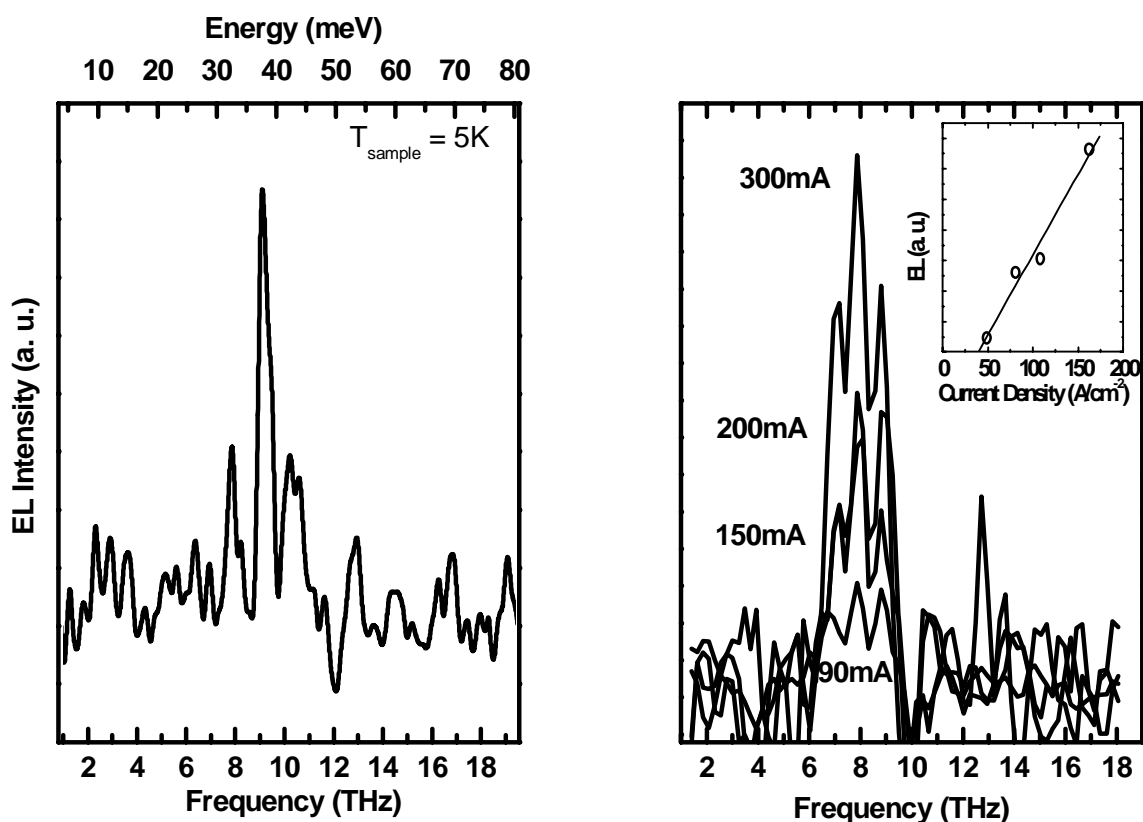


Figure 2: Measured electroluminescence spectra. **Left:** SGC396. **Right:** SGC420 for four different pumping currents. Inset: Electroluminescence intensity as a function of pumping current density.

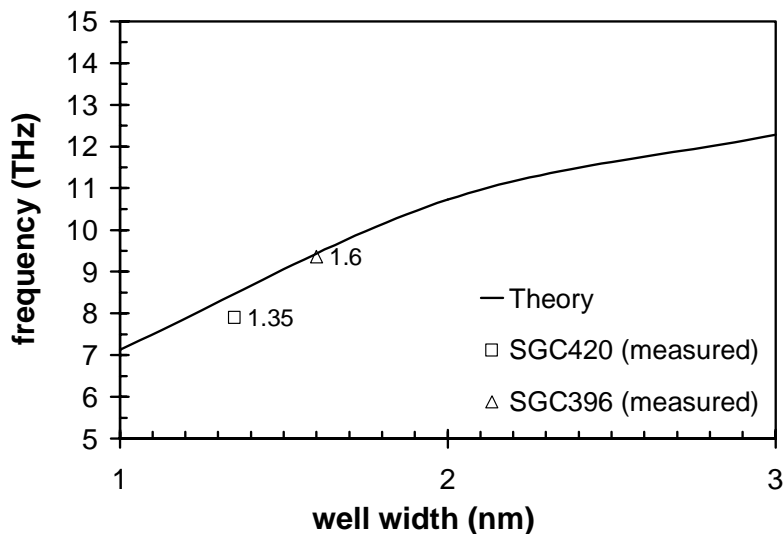


Figure 3: Center of observed electroluminescent emission versus well width (open symbols). The straight line represents the results of $k \cdot p$ calculations.

CONCLUSIONS

We have calculated the eigenenergies of holes confined by SiGe quantum wells for a variety of well widths and germanium concentrations. Samples have been fabricated according to these theoretical calculations expected to emit in the THz range. We have demonstrated electroluminescence at two different frequencies from two different SiGe/Si superlattice samples. The emission frequencies agree well with calculations, suggesting that the emission originates from transitions between confined states in the quantum wells.

The temperature dependence of the emission and its exact mechanism are currently under investigation. Samples with a larger range of well thicknesses are also under investigation.

ACKNOWLEDGEMENTS

The authors gratefully acknowledge R. Colombelli, C. Gmachl, F. H. Julien, R. W. Kelsall, J.-M. Lourtioz, E. Martinez, D. J. Paul, G. Pomrenke, L. R. Ram-Mohan, R. Soref, and G. Sun for fruitful discussions and suggestions. This work has been supported by Air Force funded DARPA contract F19628-00-C-0005 under the Terahertz program and Air Force Office of Scientific Research contract F49620-01-1-0042.

REFERENCES

1. R. A. Cheville and D. Grischkowsky, *Appl. Phys. Lett.* **67**, 1960 (1995)
2. D. M. Mittleman, M. Gupta, R. Neelamani, R. G. Baraniuk, J. V. Rudd, and M. Koch, *Appl. Phys.* **B68**, 1085 (1999)
3. K. McClatchey, M. T. Reiten, and R. A. Cheville, *Appl. Phys. Lett.* **79**, 4485 (2001)
4. R. H. Jacobsen, D. M. Mittleman, and M. C. Nuss, *Opt. Lett.* **21**, 2011 (1996)

5. D. M. Mittleman, R. H. Jacobsen, R. Neelamani, R. G. Baraniuk, and M.C. Nuss, *Appl. Phys.* **B67**, 379 (1998)
6. S. Blaser, D. Hofstetter, M. Beck, and J. Faist, *Electron. Lett.* **37** (2001)
7. D. M. Mittleman, J. Cunningham, M. C. Nuss, and M. Geva, *Appl. Phys. Lett.* **71**, 16 (1997)
8. J. Faist, F. Capasso, D. L. Sivco, A. L. Hutchinson, A. Y. Cho, *Science* **264**, 55 (1994)
9. D. Hofstetter, M. Beck, T. Aellen, J. Faist, U. Oesterle, M. Ilegems, E. Gini and H. Melchior, *Appl. Phys. Lett.* **78**, 1964 (2001)
10. M. Hass, in *Semiconductors and Semimetals* **3**, ed. R. K. Willardson and A. C. Beer (Academic Press, 1967), pp.3-16
11. M. S. Kagan, I. V. Altukhov, E. G. Chirkova, K. A. Korolev, V. P. Sinis, R. T. Troeger, S. K. Ray, and J. Kolodzey, *Proc. 10th Int. Symp. "Nanostructures: Physics and Technology"*, St. Petersburg, Russia, 445 (2002)
12. G. Dehlinger, L. Diehl, U. Gennser, H. Sigg, J. Faist, K. Ensslin, D. Grützmacher, E. Müller, *Science* **290**, 2277 (2000)
13. I. Bormann, K. Brunner, S. Hackenbuchner, G. Zandler, G. Abstreiter, S. Schmult, and W. Wegscheider, *Appl. Phys. Lett.* **80**, 2260 (2002)
14. S. A. Lynch, S. S. Dhillon, R. Bates, D.J. Paul, D. D. Arnone, D. J. Robbins, Z. Ikonic, R. W. Kelsall, P. Harrison, D. J. Norris, A. G. Cullis, C. R. Pidgeon, P. Murzyn, and A. Loudon, *Mat. Sci. Eng.* **B89**,10 (2002)
15. S. A. Lynch, R. Bates, D. J. Paul, D. J. Norris, A. G. Cullis, Z. Ikonic, R. W. Kelsall, P. Harrison, D. D. Arnone, and C. R. Pidgeon, *Appl. Phys. Lett.* **81**, 1543 (2002)
16. Quantum Semiconductor Algorithms, Inc., 5 Hawthorne Circle, Northborough, MA 01532-2711, U.S.A.
17. M. M. Rieger and P. Vogl, *Phys. Rev.* **B48**, 14276 (1993)
18. D. J. Godbey, J. V. Hill, J. Deppe, and K. D. Hobart, *Appl. Phys. Lett.* **65**, 711 (1994)
19. M. W. Dashiell, R. T. Troeger, S. L. Rommel, T. N. Adam, P. R. Berger, J. Kolodzey, A. C. Seabaugh, and R. Lake, *IEEE Trans. Electron Dev.* **47**, 1707 (2002)
20. T. N. Adam, S. Shi, S. K. Ray, R. T. Troeger, D. Prather, and J. Kolodzey, *Proc. IEEE Lester Eastman Conference on High Performance Devices*, 402 (2002)